Preparation of Novel ZSM-5 Zeolite-Filled Chitosan Membranes for Pervaporation Separation of Dimethyl Carbonate/Methanol Mixtures

Bingbing Liu,[1,2] Yiming Cao,[1] Tonghua Wang,[3] Quan Yuan[1]

[1]*Laboratory of Environmental Engineering, Dalian Institute of Chemical Physics, Chinese Academy of Sciences, Dalian 116023, China*
[2]*Graduate University of Chinese Academy of Sciences, Beijing 100049, China*
[3]*School of Chemical Engineering, Dalian University of Technology, Dalian 116021, China*

Received 22 December 2006; accepted 16 May 2007
DOI 10.1002/app.26876
Published online 23 July 2007 in Wiley InterScience (www.interscience.wiley.com).

ABSTRACT: Novel mixed matrix membranes were prepared by incorporating ZSM-5 zeolite into chitosan polymer for the pervaporative separation of dimethyl carbonate (DMC) from methanol. These membranes were characterized by scanning electron microscopy (SEM), Fourier transform infrared spectroscopy (FTIR), and X-ray diffraction (XRD) to assess their morphology, intermolecular interactions, and crystallinity. Sorption studies indicated that the degree of swelling for zeolite-filled membranes increased with zeolite content in the membrane increasing and the separation selectivity of DMC/methanol was dominated by solubility selectivity rather than diffusivity selectivity. The characteristics of these membranes for separating DMC/methanol mixtures were investigated by varying zeolite content, feed composition, and operating temperature. The pervaporation separation index (PSI) showed that 5 wt % of ZSM-5 zeolite-filled membrane gave the optimum performance in the PV process. From the temperature-dependent permeation values, the Arrhenius activation parameters were estimated. The resulting lower activation energy values obtained for zeolite-filled membranes contribute to the framework of the zeolite. © 2007 Wiley Periodicals, Inc. J Appl Polym Sci 106: 2117–2125, 2007

Key words: pervaporation; chitosan; zeolite; dimethyl carbonate; methanol

INTRODUCTION

As a green chemical intermediate, dimethyl carbonate (DMC) is a safe substitute for dimethyl sulfate and phosgene in many industrial processes due to the carbonyl and the methyl group. In addition, DMC has excellent characteristics as a fuel additive for internal combustion engines, which makes DMC especially important to the oil industry as an alternative to methyl *tert*-butyl ether (MTBE), the most widely used gasoline additive, due to environmental concerns associated with the use of MTBE.[1] DMC has more excellent characteristics as a fuel additive, including favorable distribution in gasoline/water, high oxygen content (53 wt %), good blending properties, and fast biodegradation. DMC is primarily produced on an industrial scale by oxidative carbonylation of methanol. Pacheco and Marshall[2] predicted that a substantially large scale-up of current DMC production would be needed to meet the potential market need. But, separation of DMC/methanol mixtures is difficult due to the azeotropic nature of the mixtures. Conventional separation methods including extractive distillation, pressure swing distillation, liquid–liquid extraction, adsorption on zeolites, and low temperature crystallization have been proposed to separate and purify DMC. But, all these methods consume higher energy.[2] Pervaporation (PV) appears to be a promising alternative process for DMC/methanol mixtures separation, at least as a complement to distillation that is being used in the commercial DMC manufacture.[3–5]

In the recent years, there has been increased interest in the use of the PV membrane separation process for the separation of organic liquid mixtures, since the PV technique is considered to be an energy-saving process.[6] The PV performance is mainly regulated by the physicochemical structure of the membrane rather than the vapor–liquid equilibria of the system of interest. The separation is controlled by the differences in diffusivities and solubilities of the competing components through the membrane. Because of differing permeation rates of the components, one substance at low concentration in the feed stream can be highly enriched in the permeate. Therefore, organic–organic separation is

Correspondence to: Y. Cao (ymcao@dicp.ac.cn).
Contract grant sponsor: Chinese Ministry of Science and Technology (National 973 Program); contract grant number: 2003CB615703.

Journal of Applied Polymer Science, Vol. 106, 2117–2125 (2007)

the most significant potential application for PV membrane process.

Chitosan was chosen as the PV membrane material because of its high hydrophilicity, good forming properties, functional groups that can be easily modified apart from its good mechanical, and chemical stability. Won et al.[7,8] disclosed that chitosan and crosslinked chitosan membranes were capable of separating DMC/methanol/water mixtures by PV. However, because of the close packing of polymer chains caused by intermolecular and intramolecular hydrogen bonding, the separation performance of homogeneous chitosan membrane is not satisfactory. The incorporating of zeolites or porous fillers into dense membranes can improve the separation performance of PV membranes[9,10] due to the combined effects of molecular sieving action, selective adsorption, and difference in diffusion rates. Experimental studies have shown that the incorporation of zeolites usually results in an increase of either separation factor[11–13] or flux[14–16] for many liquid separations except a few systems where both separation factor and flux have risen.[17–20] In addition, zeolites have high mechanical strength, good thermal and chemical stability and thus, the membranes filled with these zeolites, can be used over a wide range of operating conditions.

ZSM-5 zeolites having the MFI-type structures have been widely studied in membrane applications.[21–23] The straight channels in ZSM-5 zeolite are elliptical, with an opening of 0.51 × 0.57 nm, and the sinusoidal channels are almost circular, with a diameter of 0.54 nm.[24] The objective of the current work is to develop and compare the effect of adding ZSM-5 zeolite into a chitosan membrane as a filler to improve the membrane properties. Two types of chitosan membranes (homogeneous chitosan membrane and ZSM-5 zeolite filled chitosan membrane) were developed and characterized. The physicochemical changes in the obtained membranes were investigated, and the membranes were employed for the PV separation of DMC/methanol mixtures at different temperatures. The values of permeation flux, separation selectivity, and PV separation index (PSI) were evaluated and compared. From the temperature dependence of the permeation flux, the Arrhenius activation parameters were estimated.

EXPERIMENTAL

Materials

Chitosan ($\overline{M}_w \sim 200{,}000$; N-deacetylation degree 75–85%) was obtained from Sigma–Aldrich Chemicals; DMC was purchased from Fluka Chemical Company; methanol and acetic acid were purchased from Shenyang Lianbang Chemical Company (Shenyang, China); ZSM-5 zeolite with an average particle size of ~ 2 μm in powder form was kindly supplied by Dalian Institute of Chemical Physics, Chinese Academy of Sciences.

All the chemicals were of reagent grade and were used without further purification. Deionized laboratory water was used to make the aqueous solutions for membrane preparation and treatment. The feed mixtures were prepared by blending methanol and DMC with a predetermined composition.

Membrane preparation

Homogeneous dense chitosan membranes were initially prepared by solution-casting method. A preweighed chitosan powder was dissolved in 2 wt % acetic acid aqueous solution for about 24 h at room temperature to produce a casting solution consisting of 1.5 wt % chitosan. The solution was then filtered using a fritted glass disc filter to remove a trace amount of undissolved residual solids or impurities, and the solution was allowed to stand for about 12 h to remove the air bubbles. The resulting homogeneous solution was cast onto a horizontally positioned glass plate in a dust-free atmosphere at 50°C. After being dried for about 12 h, the dried membrane was subsequently peeled-off and was designated as M-0. The thickness of the membrane was measured at different points using Pocket thickness gauges electronic digital indicators (Chengdu Chengliang Tool, China), and the average thickness was considered for calculation. The thickness of the membrane was found to be 35 ± 2 μm.

For the preparation of zeolite-filled chitosan membrane, a known amount of ZSM-5 zeolite was added into a chitosan solution. The mixed solution was stirred for about 24 h and then, and it was kept in an ultrasonic bath at a fixed frequency of 40 kHz for about 30 min to improve the dispersion of zeolite in the polymer matrix. It was then filtered and left overnight to get a homogeneous solution. The resulting solution was poured onto a glass plate, and the membrane was dried as mentioned earlier. The amount of ZSM-5 zeolite with respect to chitosan was varied from 5, 10, and 15 wt %, and the membranes thus obtained were designated as M-1, M-2, and M-3, respectively.

Scanning electron microscopy

The microstructure of the membranes was examined by PHILIPS XL-30 scanning electron microscope at 15 kV accelerating voltage. The membranes were freeze-fractured in liquid nitrogen and then mounted on the aluminum stub. The specimens were sputter coated with gold prior to macroscopic observation.

The membranes were examined to determine if the zeolite particles were dispersed evenly.

Fourier transform infrared spectroscopy

The incorporation of different amounts of zeolite in chitosan was confirmed by FTIR spectroscopy (Thermo Nicolet Nexus, USA). Membrane samples were ground well to make KBr pellets under a hydraulic pressure of 600 kg/cm^2, and spectra were recorded in the range of 700–4000 cm^{-1}. In each scan, the amount of membrane sample and KBr were kept constant to estimate the changes in the intensities of characteristics peaks with respect to the amount of zeolite loading.

Wide-angle X-ray diffraction

The morphology of the pure chitosan membrane and zeolite-filled membranes was studied at room temperature using a Rigaku D/MAX advanced wide-angle X-ray diffractometer. The X-ray source was Ni-filtered Cu Kα radiation (40 kV, 100 mA). The dried membranes of uniform thickness (35 ± 2 μm) were mounted on a sample holder, and the patterns were recorded in the reflection mode at an angle 2θ over a range of 5°–45° at a speed of 5°/min.

PV separation experiments

PV separation experiments were performed in an apparatus designed indigenously. The schematic PV apparatus is shown in Figure 1. The PV apparatus consists of a stirred stainless steel cell having an effective membrane surface area of 13.85 cm^2 with a diameter of 4.2 cm, and the capacity of the feed compartment is about 250 mL. The feed solution with predetermined composition was stored in the feed tank, and the temperature of the feed mixture was kept constant using a thermostatic water jacket. A circulation pump was used to circulate the feed solution from the feed tank to the membrane cell, and the circulation rate was kept high to minimize concentration polarization in the permeation cell and to maximize mixing of the solution in the tank. The permeate side pressure was maintained at less than 10 Torr by using a vacuum pump. The test membrane was equilibrated for 2 h with the feed DMC/methanol mixtures before starting the PV experiment. After the establishment of steady state, permeate vapor was condensed and collected in a glass cold trap, which was immersed in liquid nitrogen. The permeation flux was determined gravimetrically from the weight of permeate sample collected over a given period of time per unit membrane area. The compositions of the feed and the permeate were analyzed using a gas chromatography (GC7890II, Shanghai Techcomp Instrument, China) equipped with a flame ionization detector (FID).

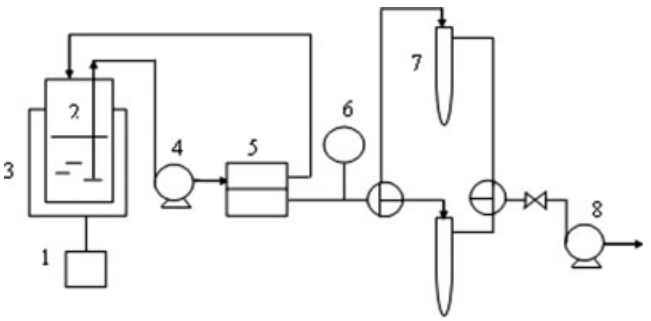

Figure 1 Schematic diagram of PV setup: (1) thermostat control, (2) feed tank, (3) heating device, (4) feed circulation pump, (5) PV cell, (6) pressure gauge, (7) cold trap, and (8) vacuum pump.

The permeation rate and permeate composition were tested periodically until a steady state of permeation was reached. Two cold traps were used alternatively during PV runs so that the membrane permselectivity could be determined without interrupting the PV operation. The results for PV separation of DMC/methanol mixtures were reproducible, and the errors inherent in the PV measurements were less than 5.0%.

PV experiments were performed for the feed mixtures ranging from 10 to 90 wt % methanol. Membrane performance in PV experiments was studied by calculating the total flux (J), separation factor (α), and PSI.[25] These were calculated, respectively, using the following equations:

$$J = \frac{W}{At} \tag{1}$$

$$\alpha = \frac{Y_{\mathrm{MeOH}}/Y_{\mathrm{DMC}}}{X_{\mathrm{MeOH}}/X_{\mathrm{DMC}}} \tag{2}$$

$$\mathrm{PSI} = J(\alpha - 1) \tag{3}$$

where W is the mass of the permeate (kg), t is the permeation time (h), A is the membrane area (m^2), Y and X are the mass fractions of the permeate and feed, respectively; subscripts MeOH and DMC denote methanol and DMC, respectively.

Swelling measurements

After being kept in desiccators to desorb any moisture absorbed from the air, the preweighed membranes were immersed in a known composition of DMC/methanol mixtures in a closed bottle at room temperature for over 48 h for an equilibrium swelling. The membranes were periodically weighed until the mass had been constant. Then, the membrane sample was taken out and wiped off the surface solution carefully with tissue paper, and weighed as quickly as possible. The amount of sorbed liquid in the mem-

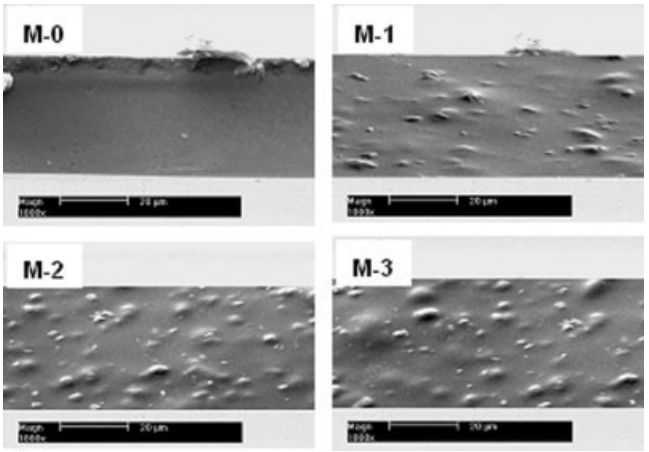

Figure 2 Cross-sectional morphology of pure and zeolite-filled chitosan membranes.

branes was expressed as the degree of swelling (DS), which was calculated using

$$\mathrm{DS}(\%) = \frac{W_s - W_d}{W_d} \times 100 \quad (4)$$

where W_s and W_d are the weights of the swollen and dry membranes, respectively.

The membranes were then immediately placed in a desorption cell connected to a cold trap that was followed by a vacuum pump. The liquid sorbed by the membranes were desorbed under vacuum and collected in the trap. The collected liquid was then weighed and analyzed for composition by gas chromatography. The individual sorbed amount was calculated from the total sorbed amount and the sorbed composition. Solubility selectivity (α_s) was calculated as follows:

$$\alpha_s = \frac{C_{\mathrm{MeOH}}/C_{\mathrm{DMC}}}{X_{\mathrm{MeOH}}/X_{\mathrm{DMC}}} \quad (5)$$

where C_{MeOH} and C_{DMC} are the weight fractions of methanol and DMC in the membrane, and X_{MeOH} and X_{DMC} are the weight fractions of methanol and DMC in the solution, respectively.

According to the solution-diffusion model, diffusivity selectivity α_D was calculated as

$$\alpha_D = \frac{\alpha}{\alpha_S} \quad (6)$$

RESULTS AND DISCUSSION

Membrane characterization

SEM studies

Figure 2 shows the cross-sectional views of the pure and zeolite-filled chitosan membranes. From the micrographs, it can be seen that the zeolite was distributed evenly in the chitosan polymer. Furthermore, the photographs clearly show that most of the zeolite crystals were embedded in the membrane matrix, with no obvious voids around them. This ensured that the zeolite-filled membranes obtained were free possible defects. The SEM micrograph was also used as a comparison to the different concentrations of ZSM-5 zeolite-filled chitosan membranes.

FTIR studies

The FTIR spectra of pure chitosan membrane and ZSM-5 zeolite-filled membranes are shown in Figure 3. Chitosan membrane showed a broad band at 3100–3500 cm^{-1} that was attributed to O—H stretching vibrations. Compared with the spectrum of chitosan membrane, the bands of zeolite-filled membranes at 3100–3500 cm^{-1} obviously broadened and shifted to lower wavenumber, and such results may be caused by the dissociation of hydrogen bonding among hydroxyl groups of chitosan. In addition, the multiple peaks appeared at around 1100 cm^{-1} are assigned to C—O stretching vibrations. The C—O at 1125 cm^{-1} for chitosan membranes shifted from 1125 to 1085 cm^{-1} for zeolite-filled membranes, indicating the formation of intermolecular hydrogen bonds between zeolites and chitosan. The small shift of zeolite-filled membranes compared with chitosan membrane was due to the decreased interaction of chitosan by filling of zeolites. These results suggested that the zeolites could also form hydrogen bonding with chitosan, which weaken the interaction of chitosan to some extent.

XRD studies

To study the effect of ZSM-5 zeolite on the membrane morphology, X-ray diffraction was employed,

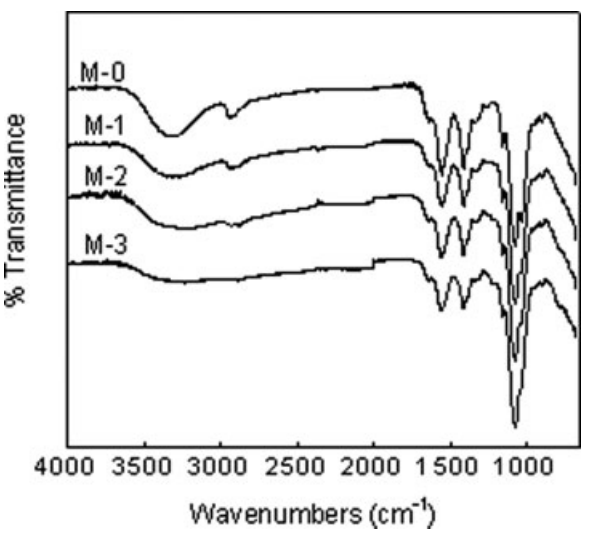

Figure 3 FTIR spectra of chitosan membranes with and without zeolite.

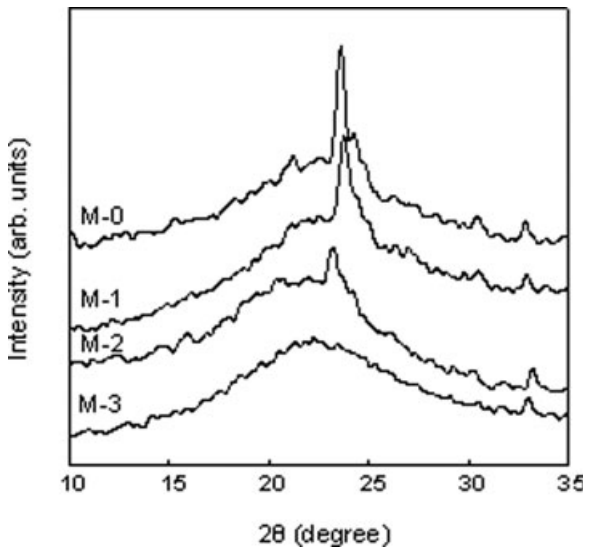

Figure 4 Wide-angle X-ray diffraction patterns for pure and zeolite-filled chitosan membranes.

and the patterns of pure chitosan membrane and zeolite-filled membranes are presented in Figure 4. The pure chitosan membrane (M-0) exhibits a typical peak that appeared at $2\theta = 23.8^\circ$, and this is in accordance with the work reported by Urbanczyk and Lipp-Symonowicz.[26] From the patterns, it is observed that the intensity of the peak became weaker after filling the ZSM-5 zeolite into chitosan. This implied that the interaction between zeolite and chitosan resulted in destroying the crystalline domain, thereby loosing the polymer-chain packing. This change facilitates methanol and DMC transport through the zeolite-filled membranes.

Effects of feed composition and zeolite loading on membrane swelling and sorption properties

In the PV process, the degree of membrane swelling is an important factor that controls the transport of permeating molecules under the chemical potential gradient.

To study the effects of the feed composition and zeolite loading on the membrane swelling, the percent DS of all the membranes was plotted as a function of different concentration of methanol in the feed mixture at 25°C as shown in Figure 5. It is observed that the DS increased for all the membranes with increasing weight fraction of methanol in the feed. Meanwhile, filling of ZSM-5 zeolite increased the DS of the membrane, which indicated that the zeolite filling significantly increased the adsorption ability of chitosan membrane toward DMC/methanol mixtures. This may be due to the introduction of the interaction between the zeolite and chitosan chains, the hydrogen bond interaction among chitosan chains weakened, which would

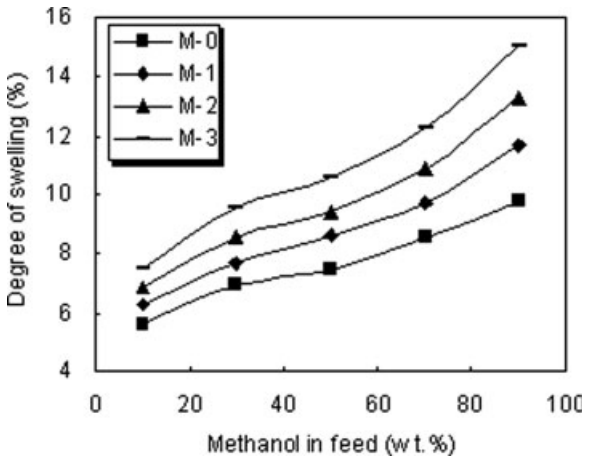

Figure 5 Variation of degree of swelling with different concentration of methanol in the feed for different content of zeolite-filled chitosan membranes.

release part of hydroxyl groups on chitosan chains. These results made the chitosan chains packing looser and the semicrystalline structure of chitosan membrane broken, which could be demonstrated by the XRD results. The looser packing structure would make chitosan chain more flexible and enhance the chain thermal motion. In addition, the decrease of chitosan membrane crystallinity would create higher free volume in the membranes. Obviously, the chain-packing relaxation and the increase of free volume were both expected for the enhanced swelling with an increase of zeolite content in the membrane.

On the basis of the sorption data, the solubility selectivity and diffusivity selectivity were calculated through eqs. (5) and (6) as shown in Figure 6. It is observed that solubility selectivity was greatly higher than the diffusivity selectivity in all the membranes, which can be concluded that the separation

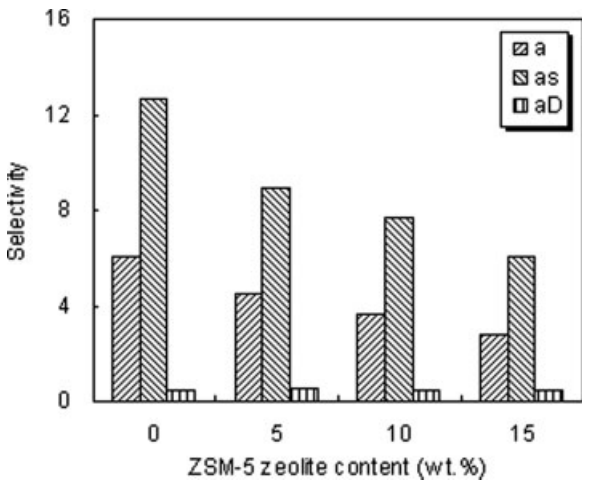

Figure 6 Variation of solubility and diffusivity selectivity with different content of zeolite-filled chitosan membranes at 70 wt % of methanol in the feed.

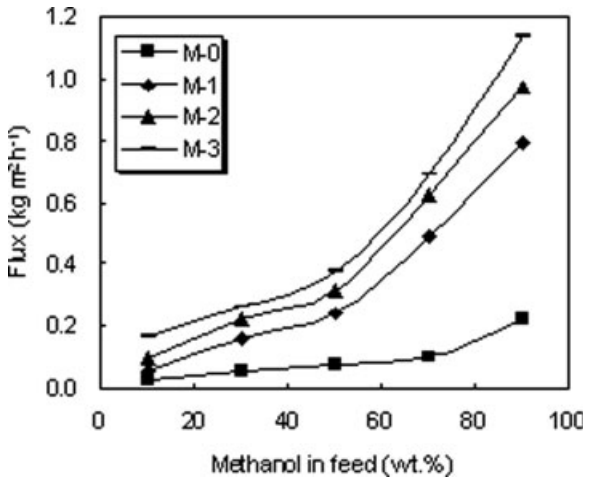

Figure 7 Variation of total flux with different concentration of methanol in the feed for different content of zeolite-filled chitosan membranes.

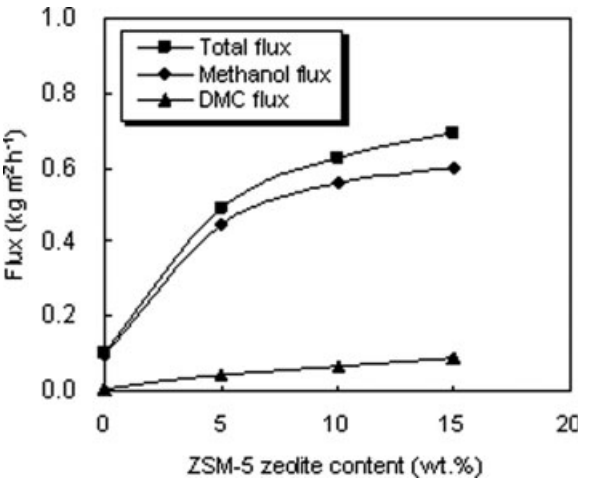

Figure 8 Variation of the total flux and the fluxes of methanol and DMC with different content of zeolite in membranes at 70 wt % methanol in the feed.

of DMC/methanol was mainly governed by solubility selectivity. But at the same time, the polymer-chain packing became more relaxed, which would weaken the solubility selectivity of membrane matrix with zeolite content increasing; moreover, the decreased solubility selectivity may be due to the low adsorptive selectivity of ZSM-5 zeolite itself.

Effects of feed composition and zeolite loading on PV properties

Figure 7 shows the effect of feed composition on the total permeation flux for all the membranes. It is found that the total permeation flux increased for all the zeolite-filled membranes with the concentration of methanol in the feed increasing and this is in accordance with the results observed in the swelling study. When the methanol concentration in the feed was higher, the amorphous region in the membrane became more swollen. Consequently, the polymer chain became more flexible and the mass transfer resistance in zeolite-filled membranes decreased, which would be advantageous for the permeation of DMC/methanol mixtures.

The efficacy of the membranes in PV process is generally assessed based on the permeation of individual components. Thus, the extent of the permeation of individual components was determined by the plotting of the total flux and the fluxes of methanol and DMC as a function of the zeolite content in the membranes with 70 wt % of methanol in the feed, as shown in Figure 8. From the plot, it is clearly noticed that the total flux and flux of methanol are close to each other; whereas, the flux of DMC is negligible for all the membranes throughout the investigated range of methanol compositions, suggesting that the membranes developed in this study are highly selective toward methanol molecules. Further, the total flux, the fluxes of methanol and DMC all increased with zeolite content in the membranes increasing, this is due to the increase of free volume and chain-packing relaxation.

The overall selectivity of a membrane in the PV process is generally explained by the interaction between the membrane and permeating molecules, the molecular size of the permeating species, and the pore diameter of the membrane. Figure 9 displays the effect of methanol concentration in the feed on the selectivity of all the membranes. It is observed that the separation factor decreased significantly for all the membranes with increasing methanol concentration in the feed. This suggests that the membrane undergoes greater swelling, owing to increased selective interaction between methanol molecules

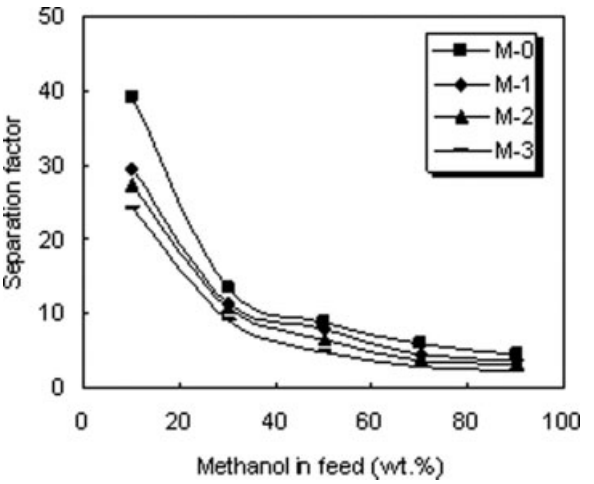

Figure 9 Variation of separation factor with different concentration of methanol in the feed for different content of zeolite-filled chitosan membranes.

TABLE I
Pervaporation Flux and Separation Factor of Different Membranes for Different Methanol Content in the Feed at 25°C

Methanol content (wt %)	J (kg m^{-2} h^{-1})				α			
	M-0	M-1	M-2	M-3	M-0	M-1	M-2	M-3
10	0.029	0.056	0.094	0.165	39.2	29.4	27.6	24.2
30	0.053	0.163	0.218	0.263	13.5	11.4	10.7	9.2
50	0.076	0.239	0.316	0.374	8.9	7.9	6.5	4.7
70	0.103	0.492	0.624	0.692	6.1	4.5	3.6	2.8
90	0.223	0.791	0.973	1.141	4.7	3.6	3.1	2.4

and the membrane. On the other hand, the separation factor decreased from membrane M-0 to M-3 upon increasing zeolite content for all the investigated methanol compositions. This is due to the increase of free volume and chain-packing relaxation with zeolite content increasing, which decreased the solubility selectivity.

The calculated results of total flux and selectivity, fluxes of methanol and DMC measured at 25°C for all the membranes in different compositions of feed mixture are presented in Tables I and II, respectively. There is a systematic increase in the total flux with respect to both the methanol concentration and zeolite loading, while the separation factor decreased with an increasing amount of the zeolite throughout the investigated range of methanol concentration. With respect to the individual fluxes, the fluxes of methanol and DMC both increased from membrane M-0 to M-3. This is due to the increase of free volume with the filling of the zeolite.

Effect of zeolite loading on PSI

The PSI is the product of total permeation flux and selectivity, which characterizes the performance of PV membranes. This index can be used as a relative guideline index for the design of PV membrane separation processes and also to select a membrane with an optimal combination of flux and selectivity. Figure 10 shows the variation of PSI as a function of ZSM-5 zeolite content in the membranes for 70 wt % of methanol in the feed at 25°C. It is observed that the PSI value increased with zeolite content in the membrane increasing, reaching a maximum at around 5 wt % of zeolite loading, and then decreased with further increase of zeolite content. High permeation flux gave a low separation factor and vice versa.[27] From Table I, the permeation flux increased from 0.103 to 0.692 kg m^{-2} h^{-1} when the zeolite content was increased from 0 to 15 wt %. However, the separation factor decreased from 6.06 to 2.81. Therefore, the calculated PSI showed that 5 wt % of ZSM-5 zeolite loading gave the optimum performance in the PV process. Meanwhile, it is also observed that the PSI value of the chitosan membrane was improved after filling the ZSM-5 zeolite. This is because the filling of the zeolite into the membrane matrix changes the membrane's structure, which may have a significant influence on membrane properties. In a word, the membranes filled with the ZSM-5 zeolite showed better PV performance for the separation of DMC/methanol mixtures.

Effect of temperature on PV properties

The temperature is an important factor affecting the PV process in all the steps: sorption, diffusion, and desorption. Generally, the flux increases as the temperature increases, and the overall temperature effect on the partial flux at a fixed condition can usually be described with an Arrhenius expression. The separation efficiency of the membrane will thus be dependent on the overall activation energy of each permeant.

The effect of operating temperature on PV properties for DMC/methanol mixtures is shown in Table III. It can be observed that permeation flux increased significantly and separation factor decreased slightly from 25 to 55°C. This was because of increasing thermal energy, which increased the free volume in the membrane matrix on account of the increased frequency and amplitude of the polymer chain jumping.[28] As a result, the diffusion of both permeating molecules increased, and this led to higher flux, whereas the selectivity was suppressed. On the other hand, with the operating temperature increasing, the vapor pressure of both methanol and DMC in the feed compartment also increased, but the vapor

TABLE II
Pervaporation Fluxes of Methanol and DMC for Different Membranes for Different Methanol Content in the Feed at 25°C

Methanol content (wt %)	J_m (kg m^{-2} h^{-1})				$J_D \times 10$ (kg m^{-2} h^{-1})			
	M-0	M-1	M-2	M-3	M-0	M-1	M-2	M-3
10	0.023	0.043	0.071	0.120	0.054	0.131	0.231	0.449
30	0.045	0.135	0.179	0.209	0.078	0.276	0.390	0.530
50	0.068	0.212	0.273	0.308	0.076	0.269	0.424	0.651
70	0.096	0.449	0.558	0.600	0.068	0.431	0.658	0.916
90	0.218	0.768	0.939	1.090	0.052	0.238	0.343	0.512

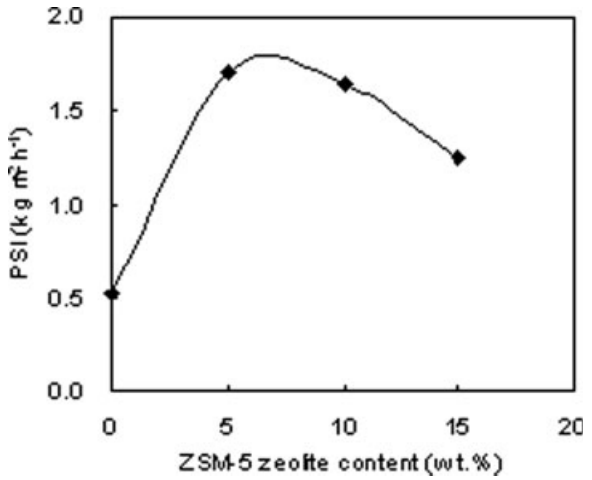

Figure 10 Variation of pervaporation separation index with different content of zeolite filled chitosan membranes at 70 wt % of methanol in the feed.

pressure at the permeate side was not affected. All this resulted in an increase in the driving force with increasing temperature.

The temperature dependence of permeation flux could be expressed by an Arrhenius-type relationship:[29]

$$X = X_0 \exp\left(-\frac{E_p}{\mathrm{RT}}\right) \tag{7}$$

where X represents permeation (J), X_0 is a constant representing pre-exponential factor (J_0), E_p represents activation energy for permeation, and RT is the usual energy term.

From the Arrhenius relationship, the PV activation energy (i.e., the energy barrier for the species to transport through the membrane) can be evaluated from eq. (7). On the basis of the respective methanol and DMC fluxes obtained at PV temperature of 25, 35, 45, and 55°C, Arrhenius plots are shown in Figures 11 and 12(A,B) for the temperature dependence of permeation flux. From a least square fit of these linear plots, the activation energies for total permeation (E_p), permeation of methanol (E_{pm}), and DMC (E_{pDMC}) were estimated, and the results were presented in Table IV.

TABLE III
Pervaporation Flux and Separation Factor of Different Membranes at Different Temperatures for 70 wt % Methanol in the Feed

Temperature (°C)	J (kg m^{-2} h^{-1})				α			
	M-0	M-1	M-2	M-3	M-0	M-1	M-2	M-3
25	0.103	0.492	0.624	0.692	6.1	4.5	3.6	2.8
35	0.150	0.597	0.727	0.729	5.3	4.3	3.3	2.6
45	0.208	0.716	0.828	0.838	4.7	3.8	3.2	2.5
55	0.270	0.818	0.946	0.987	4.3	3.7	3.1	2.4

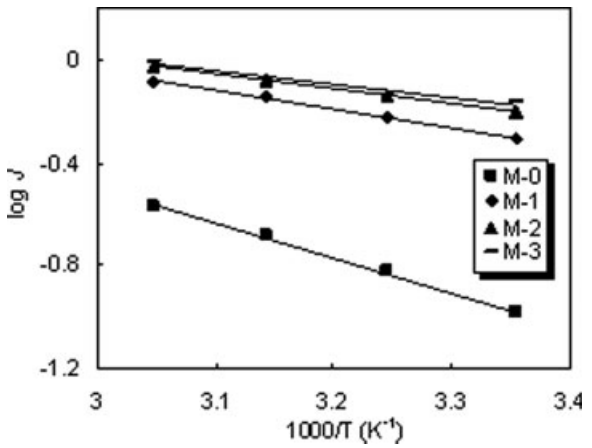

Figure 11 Variation of log J with temperature for different content of zeolite-filled chitosan membranes at 70 wt % of methanol in the feed.

From Table IV, it is noticed that the pure membrane (M-0) exhibited much higher E_p value com-

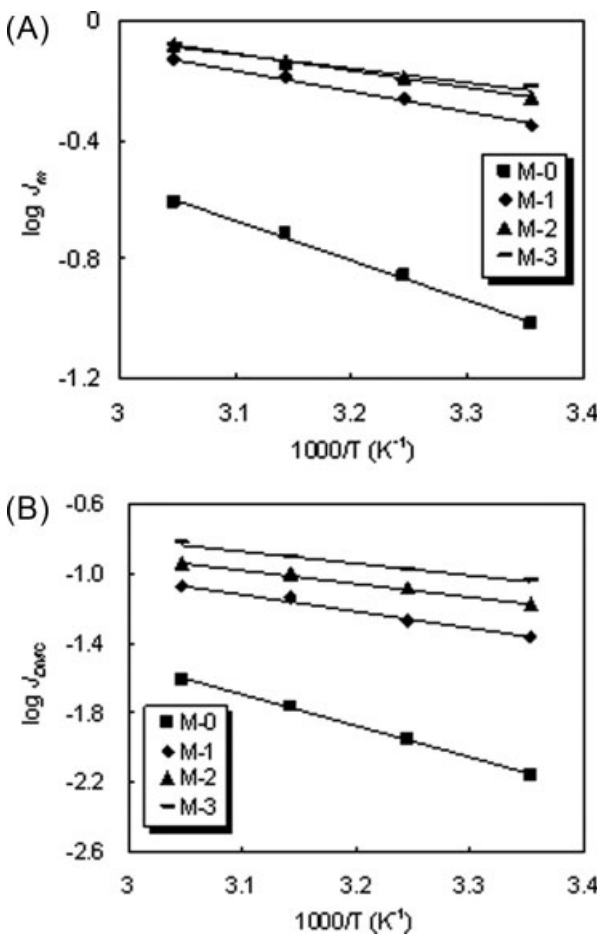

Figure 12 A and B: Variation of log J_m and J_{DMC} with temperature for different content of zeolite-filled chitosan membranes at 70 wt % methanol in the feed.

TABLE IV
Arrhenius Activation Parameters for Permeation

Parameters (kJ mol^{-1})	M-0	M-1	M-2	M-3
E_p	26.12	13.91	11.22	9.74
E_{pm}	25.37	13.39	10.76	9.10
E_{pDMC}	35.04	18.81	14.79	13.58

pared to zeolite-filled membranes (M-1 to M-3). This suggests that the permeating molecules require more energy to transport through the pure membrane due to its crystalline nature, whereas zeolite-filled membranes, molecules obviously take less energy. This is because of the molecular sieving action, which was attributed to the presence of straight and sinusoidal channels in the framework of the zeolite.[24] Therefore, E_p decreased systematically from M-1 to M-3 with increasing zeolite content. The apparent activation energy values of methanol (E_{pm}) are significantly lower than those of DMC (E_{pDMC}), suggesting that membranes have significantly higher separation efficiency.

CONCLUSIONS

Novel ZSM-5 zeolite-filled chitosan membranes were prepared for PV separation of DMC/methanol mixtures. The membranes filled with ZSM-5 zeolite have shown an improvement in the membrane performance. An increase of zeolite content in the membrane results in the increase of permeation flux and the decrease of separation factor. This was explained on the basis of the increase of free volume and chain-packing relaxation as evidenced by swelling study. The highest PV separation index was found to be 1.707 kg m^{-2} h^{-1} at 5 wt % zeolite content in the membrane for 70 wt % of methanol composition in the feed at 25°C. Temperature effect study shows the increase in permeation flux and decrease in selectivity with the temperature increasing. In comparison with the zeolite-filled membranes, the pure chitosan membrane had higher E_p values, and this signified that permeation required more energy for the transport of permeating molecules through the pure membrane because of its crystalline nature. However, the zeolite-filled membranes required less energy because of their molecular sieving action, which was attributed to the presence of straight and sinusoidal channels in the framework of the zeolite.

References

1. US Environmental Protection Agency. Fed Regist 2000, 65, 16093.
2. Pacheco, M. A.; Marshall, C. L. Energy Fuels 1997, 11, 2.
3. Mehl, W.; Scheinert, W.; Janisch, I.; Groschl, A. U.S. Pat. 5,504,239 (1996).
4. Nickel, A.; Arlt, W.; Janisch, I.; Wagner, P.; Klausener, A. U.S. Pat. 5,360,923 (1994).
5. Pasternak, M.; Bartels, C. R.; Reale, J. J. U.S. Pat. 4,798,674 (1989).
6. Rhim, J. W.; Yoon, S. W.; Kim, S. W.; Lee, K. H. J Appl Polym Sci 1997, 63, 521.
7. Won, W.; Feng, X.; Lawless, D. J Membr Sci 2002, 209, 493.
8. Won, W.; Feng, X.; Lawless, D. Sep Purif Technol 2003, 31, 129.
9. Jia, M. D.; Peinemann, K. V.; Behling, R. D. J Membr Sci 1991, 57, 289.
10. Kim, K. J; Park, S. H.; So, W. W.; Moon, S. J P. J Appl Polym Sci 2001, 79, 1450.
11. Jonquieres, A.; Fane, A. J Membr Sci 1997, 125, 245.
12. Kujawski, W.; Roszak, R. Sep Sci Technol 2002, 37, 3559.
13. Vankelecom, I. F. J.; Scheppers, E.; Heus, R.; Uytterhoeven, J. B. J Phys Chem 1994, 98, 12390.
14. Gao, Z.; Yue, Y.; Li, W. Zeolites 1996, 16, 70.
15. Okumuş, E.; Gürkan, T.; Yılmaz, L. Sep Sci Technol 1994, 29, 2451.
16. Okumuş, E.; Gürkan, T.; Yılmaz, L. J Membr Sci 2003, 223, 23.
17. Chen, X.; Ping, Z. H.; Long, Y. C. J Appl Polym Sci 1998, 67, 629.
18. Yang, H.; Nguyen, Q. T.; Ping, Z.; Long, Y.; Hirata, Y. Mater Res Innov 2001, 5, 101.
19. He, X. M.; Chan, W. H.; Ng, C. F. J Appl Polym Sci 2001, 82, 1323.
20. Kittur, A. A.; Kulkarni, S. S.; Aralaguppi, M. I.; Kariduraganavar, M. Y. J Membr Sci 2005, 247, 75.
21. Tuan, V. A.; Li, S. G.; Falconer, J. L.; Noble, R. D. J Membr Sci 2002, 196, 113.
22. Dong, W. Y.; Long, Y. C. Chem Commun 2000, 1067.
23. Vroon, Z. A. E. P.; Keizer, K.; Burggraaf, A. J.; Verweij, H. J Membr Sci 1998, 144, 65.
24. Kittur, A. A.; Kariduraganavar, M. Y.; Toti, U. S.; Ramesh, K.; Aminabhavi, T. M. J Appl Polym Sci 2003, 90, 2441.
25. Pandey, L. K.; Saxena, C.; Dubey, V. Sep Purif Technol 2005, 42, 213.
26. Urbanczyk, G. W.; Lipp-Symonowicz, B. J Appl Polym Sci 1994, 51, 2191.
27. Huang, R. M. Y.; Rhim, J. W. In Pervaporation Membrane Separation Processes; Huang, R. Y. M., Ed.; Elsevier: Amsterdam, 1991.
28. Binning, R. C.; Lee, R. J.; Jennings, J. F.; Martin, E. C. Ind Eng Chem 1961, 53, 45.
29. Huang, R. Y. M.; Yeom, C. K. J Membr Sci 1991, 58, 33.